ELSEVIER

Biophysical Chemistry 125 (2007) 151 – 158

Biophysical Chemistry

http://www.elsevier.com/locate/biophyschem

Conformations of adducts formed between the genotoxic benzo[*a*]pyrene-7,8-dione and nucleosides studied by density functional theory

Hyun Mee Lee, Youn-Hee Chae, Cheol Kwon, Seog K. Kim *

Department of Chemistry, College of Sciences, Yeungnam University, Daedong, Gyeongsan City, Gyeong-buk, 712-749, Republic of Korea

Received 27 February 2006; received in revised form 18 July 2006; accepted 18 July 2006
Available online 3 August 2006

Abstract

Benzo[*a*]pyrene (BP) is a widely distributed environmental pollutant that is metabolized by mammalian cells to a variety of genotoxic and carcinogenic intermediates that form covalent adducts with cellular DNA. One such pathway involves the metabolic activation of BP by members of the aldo-keto-reductase (AKR) family of enzymes to the highly reactive *ortho*-quinone, benzo[*a*]pyrene-7,8-dione (BPQ). This compound has been reported to react with the 2′-deoxynucleosides, dA and dG, under physiological conditions. Four BPQ–dG adducts and two –dA adducts were identified by mass spectrometry and NMR methods [Balu et al. (2004) Chem. Res. Toxicol. 17, 827–838]. However, the detailed conformations and absolute configurations around the linkage site have not been resolved. In order to determine the full conformations of these purine adducts, we carried out quantum mechanical geometry optimization using density functional theory. In the case of the BPQ–guanine adducts, six possible structures, each of which consists of two isomers, were identified. However, in the case of the adenine adducts, only four isomers were identified. The results suggest that stereoisomeric adduct pairs are expected to adopt opposite orientations with respect to the 5′→3′ direction of the modified DNA strands. The stereochemistry-dependent variations in adduct orientation may produce different biological effects, as has been observed in the case of DNA adducts derived from other metabolites of polycyclic aromatic hydrocarbons.

Keywords: Benzo[*a*]pyrene-7,8-dione; DNA; Adduct; Stereoisomer; Density functional theory

1. Introduction

Benzo[*a*]pyrene (BP) is a widely studied representative of the family of polycyclic aromatic hydrocarbons that are products of fossil fuel combustion and are thus widely distributed environmental pollutants [1]. Significant levels of BP are also present in tobacco smoke, in many common foods, and in automobile exhausts. It is well known that BP can induce cancer in animals and is suspected to be a carcinogen in humans as well. While BP itself is relatively insoluble in aqueous solutions and does not chemically react with DNA, it is metabolized to a variety of carcinogenic derivatives, including (±)-*anti*-7,8-dihydroxy-9,10-epoxy-7,8,9,10-tetrahydrobenzo[*a*]pyrene ((±)-*anti*-BPDE) [2–5]. Other metabolic routes of activation include the generation of BP radical cations that arise from a one-electron oxidation at the C6 position of BP [6–8], and the enzymatic conversion of BP to 7,8-dihydroxy BP by members of the aldo-keto-reductase family of enzymes (AKR) and their oxidation to the highly reactive *ortho*-quinone, benzo[*a*]pyrene-7,8-dione (BPQ, Fig. 1(a)) [9–12]. The diol epoxides *anti*-BPDE react chemically with DNA by forming predominantly N^2-deoxyguanosine adducts [2–5], while the radical cation forms depurinating adducts at the N7 position of adenine and guanine and the C8 position of guanine [6,8].

DNA damage associated with BP metabolites generated by the AKR pathway, including the formation of DNA adducts and oxidative DNA damage, has been reported [12,13]. It has been shown that BPQ can form stable cyclic adducts by reaction with 2′-deoxyguanosine (dG) and 2′-deoxyadenosine (dA) in aqueous solutions under physiological conditions, and the chemical structures of these nucleoside adducts have been established by NMR and mass spectrometry methods [14]. The reaction of BPQ with dG affords four unique Michael

* Corresponding author. Tel.: +82 53 810 2362; fax: +82 53 815 5412.
E-mail address: seogkim@yu.ac.kr (S.K. Kim).

0301-4622/$ - see front matter © 2006 Elsevier B.V. All rights reserved.
doi:10.1016/j.bpc.2006.07.015

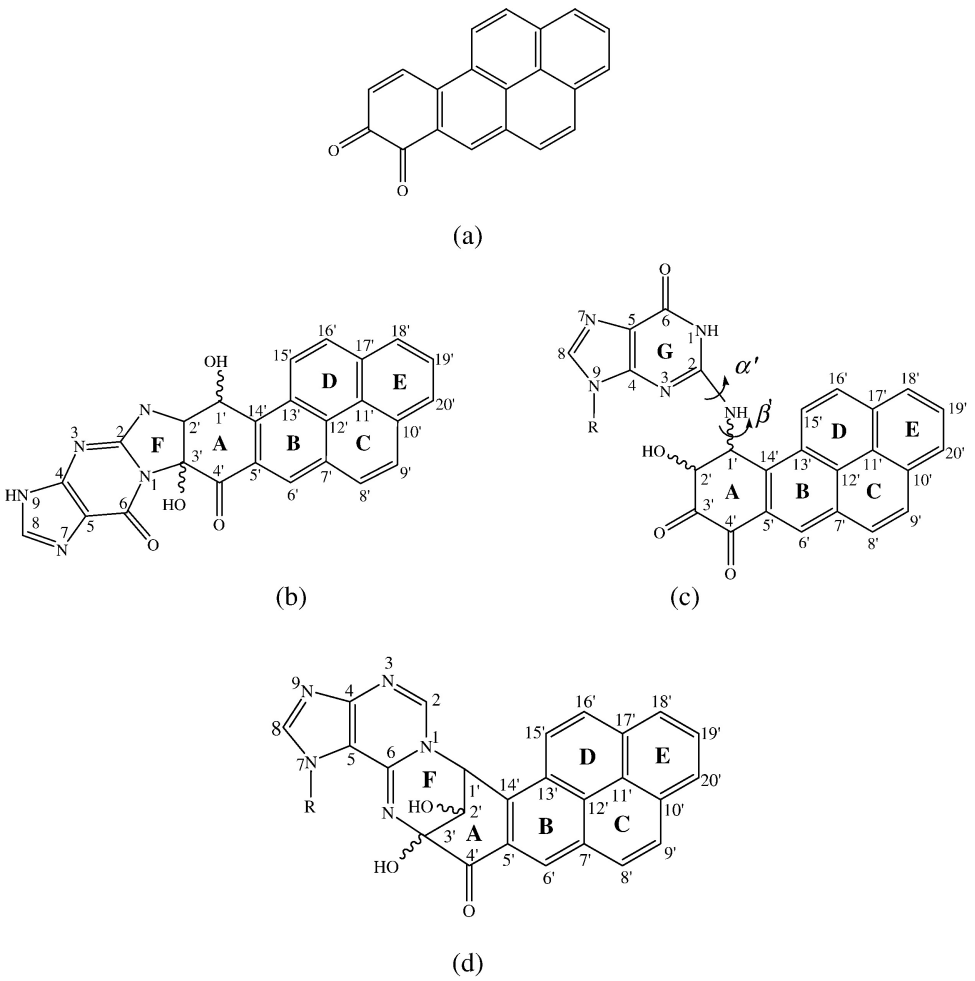

Fig. 1. Structure of the BPQ and BPQ–nucleoside adducts: (a) BPQ, (b) BPQ–$G^{1,2}$, (c) BPQ–$G^{3,4}$, (d) BPQ–$A^{1,2}$. Numbering and the marks for the atoms and the rings in this work are also shown.

addition products: a set of two diastereomers, 8-N^1,9-N^2-deoxyguanosyl-8,10-dihydroxy-9,10-dihydrobenzo[*a*]pyrene-7(8H)-one (BPQ–$dG^{1,2}$), and 10-(N^2-deoxyguanosyl)-9,10-dihydro-9-hydroxy benzo[*a*]pyrene-7,8-dione (BPQ–$dG^{3,4}$). Reactions of BPQ with dA adducts produce only one diastereomeric pair of adducts identified as 8-N^6,10-N^1-deoxyadenosyl-8,9-dihydroxy-9,10-dihydrobenzo[*a*]pyrene-7(8H)-one (BPQ–$dA^{1,2}$) [14]. The chemical structures and numbering schemes of the BPQ–guanine (BPQ–G) and the adenine (BPQ–A) adducts are depicted in Fig. 1b and c. Although the chemical structures of the BPQ–G and –A adducts were identified, detailed information regarding the conformations around the linkage site of these stereoisomeric adducts have not been studied. The absolute configuration of the substituents at the chiral carbon centers may contribute to the processing of such adducts in DNA by polymerases and DNA repair proteins. We have therefore investigated the conformational characteristics of the cyclic BPQ–A and BPQ–G adducts using density functional theory, an approach that was successfully used to delineate the absolute configurations of several structurally related equine estrogen-nucleoside adducts [15].

2. Computational methods

2.1. Starting conformations

Based on the structural characterization of the BPQ–nucleosides adducts [14], we constructed various possible initial models for the BPQ–G and –A adducts using Hyperchem 7.0 program. The geometry of BPQ was obtained by quantum mechanical calculations. The initial structures of the five-membered F ring and the adjacent A ring were constructed from all the feasible conformational families for each stereoisomeric BPQ adduct with the assistance of hand models. The chemical structure of the BPQ–$G^{1,2}$ adduct, which involves the formation of a five-membered ring between guanine and BPQ, suggests that four diastereomers are possible, which are denoted by BPQ–$G^{1,2}$–A, –B, –C, and –D (Fig. 2(a)). Similarly, in the case of the BPQ–$G^{3,4}$ adduct, in which the amine group of G and BPQ form a chemical bond, four diastereomeric adducts are possible (Fig. 2(b)). The four possible stereoisomeric BPQ–A adducts are also depicted in Fig. 2(c). In the case of the guanine–BPQ cyclic adducts (BPQ–$G^{1,2}$), stereoisomers with H and OH at the C2′ and C3′ positions in the *trans*

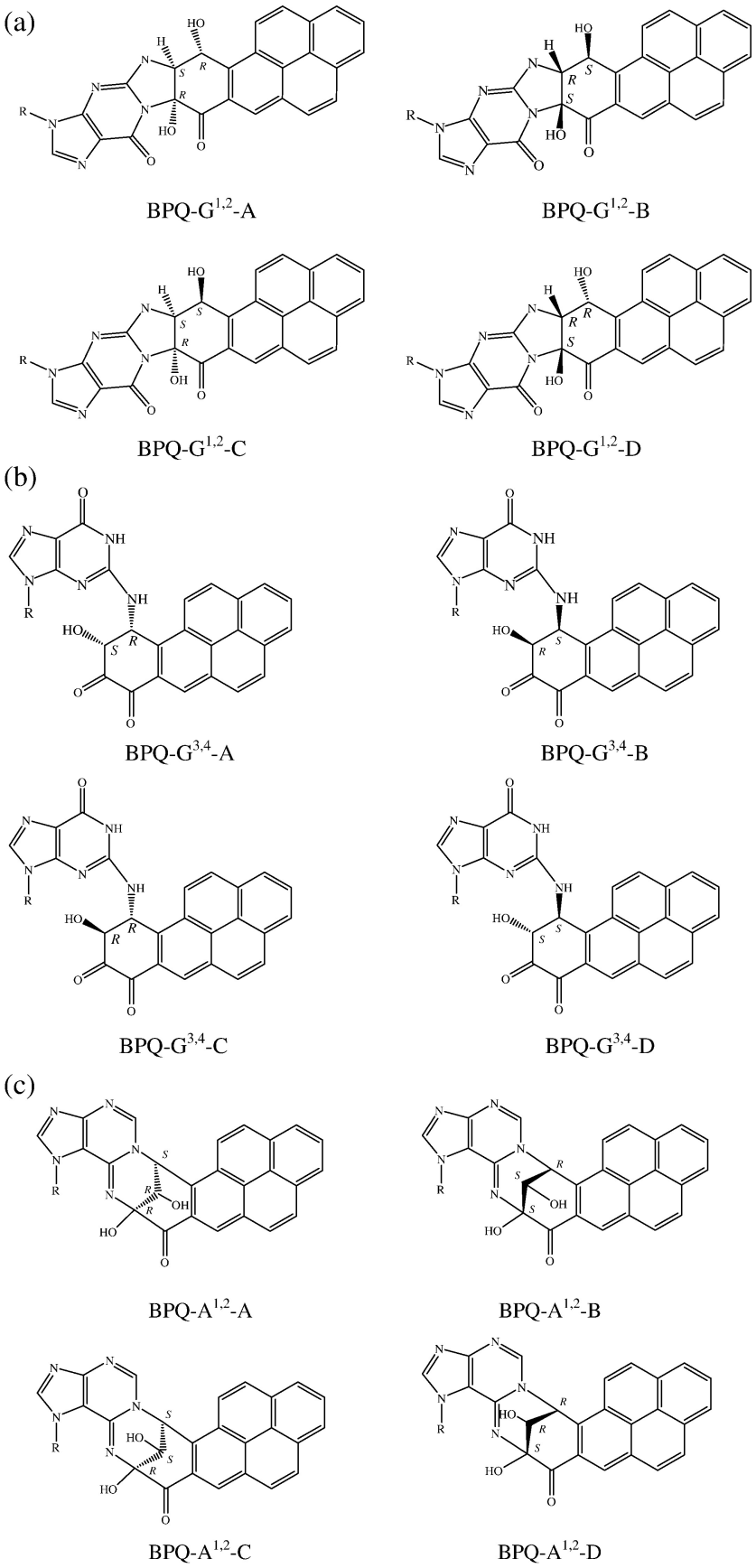

Fig. 2. Possible stereoisomeric structures of the BPQ–$G^{1,2}$ (a), BPQ–$G^{3,4}$ (b) and BPQ–$A^{1,2}$ (c) adducts.

configurations were not found, presumably because these orientations would involve a highly strained five-membered F ring (Fig. 1). For similar reasons, BPQ–A adducts other than those shown in Fig. 2(c) were not possible.

2.2. Energy computation

Energy minimizations were carried out using the AMBER force field implemented in Hyperchem 7.0. The quantum mechanical calculations were performed with Gaussian 98 software [16] using B3LYP density functional theory with the 6-31G* basis set [17–20]. The global minimum geometries for the various structures were calculated by vibrational frequency analysis. The optimized structures did not have imaginary frequencies thus indicating that local minima were identified. Computations were carried out on an IBM p690 system in the supercomputer center of the Korea Institute of Science and Technology Information (KISTI).

3. Results

3.1. BPQ–G adducts

As mentioned above, there are four BPQ–$G^{1,2}$ stereoisomeric adducts (Fig. 2(a)). There are different conformers in each case due to the chiral carbon centers at positions C1′, C2′, and C3′ (Fig. 1). Since *trans* configurations of C2′–H and C3′-OH are not possible [15], we constructed four starting structures for each of the four stereoisomers, resulting in 16 starting structures for model building.

Table 1
Torsion angle of BPQ–$dG^{1,2}$ adducts for starting structures (deg)

		I	II	III	IV
BPQ–$dG^{1,2}$–A	α	−20.8	24.4	−0.5	5.6
	β	−28.9	31.3	−0.2	−.06
	γ	−4.4	−6.2	15.9	36.8
	δ	52.8	81.7	54.3	0.1
	ε	−102.3	−162.2	−107.9	−63.4
BPQ–$dG^{1,2}$–B	α	−25.7	20.6	−0.3	−9.6
	β	−32.3	29.0	−0.8	−3.4
	γ	−8.0	3.4	39.7	−37.9
	δ	−86.0	−51.7	−100.0	0.4
	ε	166.4	101.0	168.6	65.5
BPQ–$dG^{1,2}$–C	α	−24.0	26.0	−1.4	−1.7
	β	−31.1	38.0	−1.0	3.4
	γ	16.2	−14.8	35.0	−37.6
	δ	−83.1	−46.0	−71.5	−34.2
	ε	42.7	−43.3	22.2	−36.2
BPQ–$dG^{1,2}$–D	α	−27.4	31.7	−3.8	−5.4
	β	−30.8	35.0	2.9	−1.5
	γ	12.9	6.6	−38.6	24.4
	δ	15.9	116.5	106.9	59.6
	ε	69.4	−48.9	−44.9	57.9

α: N^2–C2′–C3′–N1.
β: C1′–C2′–C3′–C4′.
γ: C3′–C4′–C5′–C14′.
δ: C13′–C14′–C1′–$O^{1\prime}$.
ε: N^2–C2′–C1′–$O^{1\prime}$.

Table 2
Convergence of starting structures to final optimized structures

Starting structure		Optimized structure	Shape
BPQ–$G^{1,2}$–A	I	BPQ–$G^{1,2}$–A (a)	L
	II	BPQ–$G^{1,2}$–A (a)	L
	III	BPQ–$G^{1,2}$–A (a)	L
	IV	BPQ–$G^{1,2}$–A (b)	Stair
BPQ–$G^{1,2}$–B	I	BPQ–$G^{1,2}$–B (a)	L
	II	BPQ–$G^{1,2}$–B (b)	Stair
	III	BPQ–$G^{1,2}$–B (a)	L
	V	BPQ–$G^{1,2}$–B (b)	Stair
BPQ–$G^{1,2}$–C	I	BPQ–$G^{1,2}$–C (b)	Stair
	II	BPQ–$G^{1,2}$–C (a)	L
	III	BPQ–$G^{1,2}$–C (b)	Stair
	IV	BPQ–$G^{1,2}$–C (a)	L
BPQ–$G^{1,2}$–D	I	BPQ–$G^{1,2}$–D (a)	L
	II	BPQ–$G^{1,2}$–D (b)	Stair
	III	BPQ–$G^{1,2}$–D (b)	Stair
	IV	BPQ–$G^{1,2}$–D (a)	L

The dihedral angles between the five-membered F ring and cyclohexene ring (ring A) of BPQ of each of the starting structures are listed in Table 1. In this table, the designations A, B, C and D indicate different stereoisomers (Fig. 2), while the Roman numerals I, II, III, and IV represent the different initial structures that are function of different combinations of the five dihedral angles α through ε. These sets of angles define the relative conformations of the F and the A ring. The torsion angles α through δ define the relative orientation of the five-membered ring (F), the linker between the F and A rings, the A ring, and the O1′–O1′H on the A ring, respectively α(N^2–C2′–C3′–N1), β(C1′–C2′–C3′–C4′), γ(C3′–C4′–C5′–C14′), and δ(C13′–C14′–C1′–$O^{1\prime}$). The angle ε (N^2–C2′–C1′–$O^{1\prime}$) defines the spatial relationship between the F and A rings. The F ring in the starting conformation I (as defined in Table 1) of the BPQ–$G^{1,2}$ adducts has a negative α value. The angle β is also negative and the C2′ atom is out of plane. In contrast to the conformation of I, both α and β of conformation II are positive in sign with the F ring oriented on the opposite side. In conformations III and IV, the F ring is nearly planar because the angles α and β are close to zero.

The 16 starting structures converge to 8 final structures (Table 2). For instance, starting conformers, BPQ–$G^{1,2}$–A (I, II and III) (Table 1) converge to optimized conformation BPQ–$G^{1,2}$–A (a), and BPQ–$G^{1,2}$–A (IV) to BPQ–$G^{1,2}$–A (b). The resulting torsion angles are summarized in Table 3 and the stereo views of each conformer, which can be classified as "L-shaped" and "stair conformation", are depicted in Fig. 3. Both torsion angles α and β are about ±10° for all conformers, indicating that the F ring is close to being planar. The angle γ lies between −45.0° and 47.0° for all conformers. The angle δ of the L-shaped BPQ–$G^{1,2}$–A and BPQ–$G^{1,2}$–B adducts, representing the relative orientation of $O^{1\prime}$–$HO^{1\prime}$ group, is about 100°, irrespective of the sign. On the other hand, the value of this angle is about 10° in the stair conformation. In the L shape, the angle ε is −158.8°∼176.6°, indicating an *anti* configuration between $C^{1\prime}$ and $O^{1\prime}$. The value of this angle for

Table 3
Torsion angles of BPQ–$G^{1,2}$ adducts for optimized structures (deg)

Adducts		I	II	III	IV
BPQ–$dG^{1,2}$–A	α	5.0	−5.3	−1.2	8.2
	β	10.4	−1.1	−1.8	4.7
	γ	−38.8	−39.4	−42.7	46.3
	δ	104.8	105.4	102.0	8.3
	ε	−176.2	−165.3	−158.8	−71.9
BPQ–$dG^{1,2}$–B	α	5.4	−8.6	6.1	−11.1
	β	1.4	−5.1	1.3	−10.6
	γ	39.6	−44.9	44.5	−38.2
	δ	−105.7	−9.0	−116.7	−10.1
	ε	165.6	73.1	176.6	72.9
BPQ–$dG^{1,2}$–C	α	−5.3	−2.6	3.4	−2.6
	β	−1.8	0.6	2.5	0.6
	γ	45.0	−41.5	47.0	−41.5
	δ	−105.5	−10.6	−118.7	−10.5
	ε	44.2	−61.4	47.0	−61.5
BPQ–$dG^{1,2}$–D	α	−3.3	5.3	5.3	−7.0
	β	−7.6	1.8	1.8	−6.6
	γ	35.6	−45.0	−45.0	43.0
	δ	9.0	105.5	106.0	5.9
	ε	64.9	−44.2	−44.3	65.0

the stair conformation is −71.9°∼73.1° which corresponds to a *gauche* conformation. In contrast, in the case of the BPQ–$G^{1,2}$–C and BPQ–$G^{1,2}$–D isomers, the value of δ suggests an equatorial conformation for the L-shaped, and an axial conformation for the stair-shaped conformation. The range of ε values is 44.2°∼65.0° (*syn* conformation) for both the L-shaped and the stair conformations, which is also in contrast to the values for the BPQ–$G^{1,2}$–A and BPQ–$G^{1,2}$–B conformers. The total energies of the eight conformers are summarized in Table 4. The energies of the L-shaped BPQ–$G^{1,2}$–A and BPQ–$G^{1,2}$–B are the lowest among all of the conformers. The energies of the L-shaped BPQ–$G^{1,2}$–C and BPQ–$G^{1,2}$–D stereoisomers are higher by ∼3.0 kcal/mol than the energies of the A and B conformers. In the stair conformation, the total energy is 4.4 kcal/mol and 2.3 kcal/mol higher for the BPQ–$G^{1,2}$–C and –D conformers, respectively, than the energies of the BPQ–$G^{1,2}$–A and –B conformers.

Table 4
The relative stereoisomer stabilities of BPQ–base adduct[a]

	Adducts	−A	−B	−C	−D
Δ*E* (kcal/mol)	BPQ–$G^{1,2}$ [b]	0	0	2.75	2.75
	BPQ–$G^{1,2}$ [c]	4.38	4.38	2.27	2.27
	BPQ–$G^{3,4}$	0	0	3.86	3.86
	BPQ–$A^{1,2}$	0.03	0.03	0	0

[a] The lowest energy of BPQ–base adducts are assigned $\Delta E=0$, and the energies are relative to this lowest energy adduct. For the BPQ–$G^{1,2}$, BPQ–$G^{3,4}$ and BPQ–$A^{1,2}$ adducts, $\Delta E=0$ corresponds to a calculated absolute energy of −964 109.28 kcal/mol, −964 106.13 kcal/mol and −916 891.01 kcal/mol, respectively.
[b] The average energies of "L" shape for BPQ–$G^{1,2}$ conformer.
[c] The average energies of "stair" shape for BPQ–$G^{1,2}$ conformer.

In the 10-(N^2-deoxyguanosyl)-9,10-dihydro-9-hydroxybenzo[*a*]pyrene-7,8-dione (BPQ–$G^{3,4}$) adducts case, the BPQ

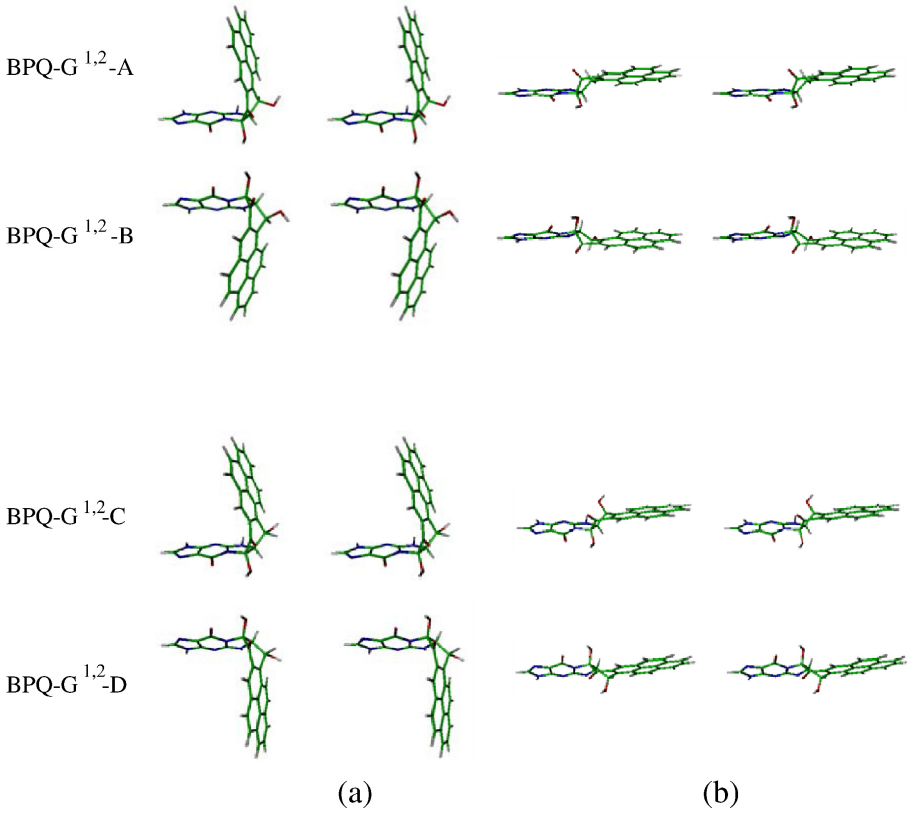

Fig. 3. Stereo views of optimized conformation for the BPQ–$G^{1,2}$ adducts. The conformations shown in (a) are denoted as "L" shape and (b) as "stair" shape.

Table 5
Torsion angles of optimized structures for BPQ–$G^{3,4}$ adducts (deg)

Torsion angle	BPQ–$G^{3,4}$–A	BPQ–$G^{3,4}$–B	BPQ–$G^{3,4}$–C	BPQ–$G^{3,4}$–D
α'	23.3	20.4	13.3	19.2
β'	103.2	234.9	76.1	239.3

and G moieties are connected by a single bond from N^2 of the purine to the C1′ site of the BPQ residue, and is thus similar to the *anti*-BPDE-N^2-dG adducts that are derived from the diol epoxide activation pathway. These adducts are expected to be conformationally far less flexible than the BPQ–$G^{1,2}$ adducts because both the guanine and the pyrenyl residues are planar and rigid, and only a little conformational flexibility is allowed with respect to the torsion angles defined in Fig. 1(c). Therefore, calculations were performed only for the four stereoisomers (Fig. 2(b)), but allowing these two torsion angles to vary. Two torsion angles α', β' values of this BPQ–$G^{3,4}$ adducts are shown in Table 5. The resulting angles of the BPQ–$G^{3,4}$ adducts are quite similar to the BPDE-N^2-dG adducts which was reported by Broyde and her coworkers [21–24]. As it is shown in Fig. 4, the BPQ–$G^{3,4}$–A and BPQ–$G^{3,4}$–B adducts on the one hand, and the BPQ–$G^{3,4}$–C and BPQ–$G^{3,4}$–D adducts on the other, are near-mirror images of one another. For examples, BPQ–$G^{3,4}$–A adducts has the same absolute configurations at the C1′ and C2′ positions as the (+)-*cis*-BPDE-N^2-dG adduct, BPQ–$G^{3,4}$–B = (−)-*cis*-BPDE-N^2-dG, BPQ–$G^{3,4}$–C = (−)-*trans*-BPDE-N^2-dG, and BPQ–$G^{3,4}$–D = (+)-*trans*-BPDE-N^2-dG adducts. In the BPQ–$G^{3,4}$ adducts case, the energy of the BPQ–$G^{3,4}$–A, BPQ–$G^{3,4}$–B is the same and lower by 3.9 kcal/mol than that of the BPQ–$G^{3,4}$–C and BPQ–$G^{3,4}$–D adducts. The hydrogen bond between N^1′H of the link and O2′ atom of A ring may be the reason for the lower energy. In the BPQ–$G^{3,4}$–C, BPQ–$G^{3,4}$–D adducts, the O^2′ atom of the A ring is directly opposite from N^1′H of the link, which makes it hard to form a hydrogen bond.

3.2. BPQ–A adducts

The linkage between BPQ and the adenine residue in the BPQ–$A^{1,2}$ adducts is a bicycle[3,3,1]nonane type ring (Fig. 2(c)). The torsion angles of the cyclohexene moiety that formed between C1′–N1–C6–N^6 of adenine and C1′–C14′–C5′–C4′ are close to zero, indicating that the two connecting rings are partially planar. In the connecting ring, only the C1′–C2′–C3′ part is puckered. The flexibility and rotational freedom in the BPQ–$A^{1,2}$ adducts is minimal, hence the calculation and the resulting structures are relatively simple as compared to the BPQ–$G^{3,4}$ adducts. The results, which are depicted in Fig. 4, show that the optimized structures of the BPQ–A adducts consist of four conformations: a set of stereoisomeric BPQ–$A^{1,2}$–A and BPQ–$A^{1,2}$–B adducts, and another set of stereoisomeric BPQ–$A^{1,2}$–C and BPQ–$A^{1,2}$–D adducts. In the BPQ–A adducts, the angle of the BPQ molecular plane relative to the planar moiety of the A residue is about 110°. The energies of the BPQ–$A^{1,2}$–C and –D conformers are very close in value to those of the –A and –B conformers.

3.3. Conformation of BPQ–G adducts

Four possible starting structures were modeled for the four stereoisomeric BPQ–$G^{1,2}$ adduct and optimizations of each were performed. As a result, L-shaped and stair-shaped conformation was found for each stereoisomer. In the L-shaped structure, the angle between the planar portion of the BPQ and the plane of the guanine residue is about 80°. Determining either L shape or stair conformation depends on the δ and ε values which represent the orientation of C^1′OH group and the relationship between the F and the A ring. Other torsion angles namely the α, β, and γ values are similar for the L-shaped and stair conformation, and thus do not play any role in determining the molecular shape (Table 3). In the case of the BPQ–$G^{1,2}$–A and –B adducts, when the δ value is about 10°, disregarding the sign, the conformation is stair-like in which the hydroxyl group is equatorial (Fig. 3). On the other hand, the molecular shape is L type with axial hydroxyl groups when the absolute δ value is above 100° (Fig. 3). The configuration of the F and A ring, represented by the ε values, is *anti* for the L shape, while it is *gauche* for the stair conformation. The BPQ–$G^{1,2}$–A and BPQ–$G^{1,2}$–B adducts are mirror images in both the L and stair conformations. The relationship between the δ value and the overall conformation of the BPQ–$G^{1,2}$–C and BPQ–$G^{1,2}$–D adducts is different from those in the BPQ–$G^{1,2}$–A and BPQ–$G^{1,2}$–B type adducts. When the δ value is about 10° with the axial hydroxyl group, the overall molecular shape is a stair

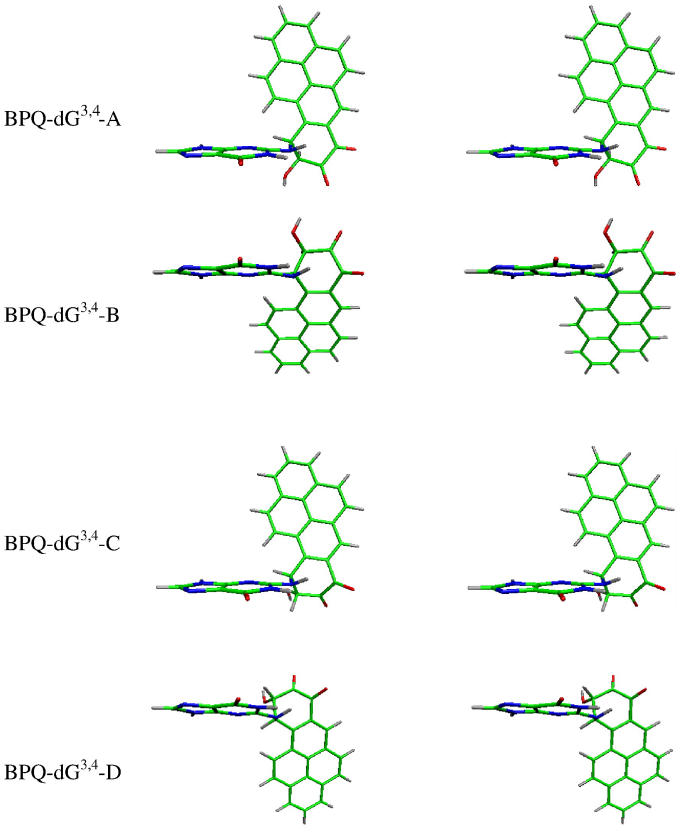

Fig. 4. Stereo views of optimized conformation for the BPQ–$G^{3,4}$ adducts.

conformation (Fig. 3), while it is L-shaped when the δ value is above 100°. The ε values of the BPQ–$G^{1,2}$–C and BPQ–$G^{1,2}$–D adducts are also different from those of the BPQ–$G^{1,2}$–A and BPQ–$G^{1,2}$–B type adducts: it is *gauche* for the L-shaped and is *anti* for the stair conformation. The BPQ–$G^{1,2}$–C and BPQ–$G^{1,2}$–D adducts are also mirror images of one another if the sugar residues are not taken into account. BPQ–$G^{3,4}$ adducts represented similar results for stereochemically similar *anti*-BPDE-N^2-dG adducts. This is because only the substituents at the C1′ and C2′ position of these BPDE-N^2-dG adducts influence the steric hindrance and orientation effects.

3.4. Conformation of BPQ–A adducts

Little flexibility is allowed for the BPQ–A stereoisomers due to the conjugated adenine moiety, sp^2 hybridization of C4′, C5′, and C14′ in the cyclohexene A ring, and the rigidity of the C1′–C2′–C3′ bridge. It can be noticed also that the conjugation between the aromatic B ring and the carbonyl group in the cyclohexene A ring contributes to the stability of these adducts. The overall shape of the optimized structure of BPQ–A adducts is the opened L shape. The angle between the molecular planes of BPQ and A is 110°, which is in contrast with the angle of 80° of the L-shaped BPQ–$G^{1,2}$ adducts.

Larger angles are due to the sp^3 orbitals of C1′ and C3′ atoms linking BPQ and adenine in comparison with the boat shape of cyclohexene in the BPQ–$G^{1,2}$ adducts. The BPQ–$A^{1,2}$–A and BPQ–$A^{1,2}$–B adducts on the one hand, and the BPQ–$A^{1,2}$–C and BPQ–$A^{1,2}$–D adducts on the other, are near-mirror images of one another (Fig. 5). Although the adducts BPQ–$A^{1,2}$–A and BPQ–$A^{1,2}$–B seem to be similar to BPQ–$A^{1,2}$–C and BPQ–$A^{1,2}$–D adducts, the orientation of the C2′-OH group in the bridge is almost parallel to the molecular plane of adenine in the latter two adducts.

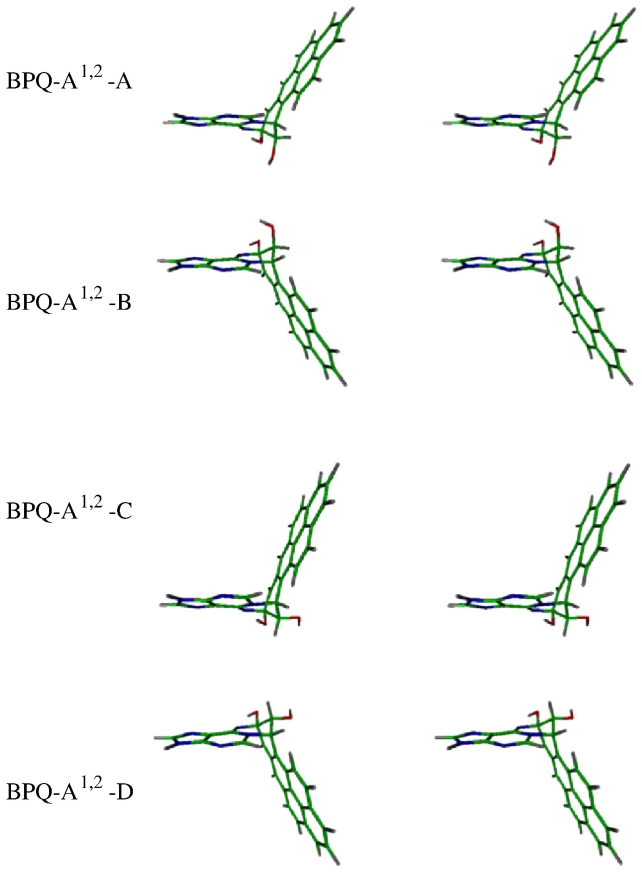

Fig. 5. Stereo views of optimized conformation for the BPQ–$A^{1,2}$ adducts.

3.5. The energies of BPQ–G and –A adducts

The most probable structure for the stereoisomers can be suggested by comparing the relative energies. The total energy of the L shape of the BPQ–$G^{1,2}$–A, –B isomers is lower by 4.4 kcal/mol as compared to the stair conformations, while in the BPQ–$G^{1,2}$–C, –D adducts case, the energy of the stair conformation is lower by 0.48 kcal/mol than L shape with RT being ~0.6 kcal/mol, this difference of 0.5 kcal/mol seems hardly significant. Therefore, the BPQ–$G^{1,2}$–A, –B isomers are likely to exist in the L shape. The stair conformation may be somewhat more stable for the BPQ–$G^{1,2}$–C, and –D adducts. The total energy of the BPQ–$A^{1,2}$–A and BPQ–$A^{1,2}$–B adducts is the same and that of the BPQ–$A^{1,2}$–C and BPQ–$A^{1,2}$–D is equal. The difference in the energy between the groups of the stereoisomers is negligible, being 0.03 kcal/mol. The only difference between the BPQ–$A^{1,2}$–A and BPQ–$A^{1,2}$–B adducts and BPQ–$A^{1,2}$–C and BPQ–$A^{1,2}$–D adducts is the direction of C2′–OH group, which is not expected to result in large energy difference.

3.6. Implications for the DNA–BPQ adduct structure

In general, all adducts discussed above significantly perturb the Watson–Crick hydrogen bonding sites of the modified nucleobases. The BPQ is directed in opposite sides relative to the plane of the base in the stereoisomer pairs of the L shape. Therefore, in native DNA, it would probably be located in the minor groove, directed in the 5′ or 3′ direction along the modified strand. It is clear that the L-shaped adducts can not intercalate between the DNA base pairs. Although the steric hindrance of BPQ seem to be less in the stair conformations as compared to the L shape, intercalation may also be impossible because the molecular plane of BPQ is displaced relative to the modified base and such a staggered adduct may have difficulty fitting into an intercalation pocket, although it is parallel to the nucleobase. As shown in Figs. 4 and 5, the bulky BPQ moiety could fit in the minor groove of double-stranded DNA.

4. Conclusion

The conformations of all the BPQ–G and BPQ–A adducts can be roughly categorized into L shape and stair conformation although some variations were found. Both L-shaped and stair conformation are possible for the BPQ–$G^{1,2}$ adducts while only opened L shape was found for the BPQ–$A^{1,2}$ adducts. Intercalation of the L-shaped adducts does not appear to be

possible. Considering the conformation of the BPQ relative to the nucleobases, BPQ may be located along the minor groove of double-stranded DNA in the BPQ–$G^{3,4}$ adduct case, while it may be located outside of the minor groove in the other L-shaped adduct including BPQ–$G^{1,2}$ and BPQ–$A^{1,2}$ adducts.

Acknowledgement

This work was supported by the Korea Research Foundation (Grant No. KRF-2005-050-C00003).

References

[1] IARC, IARC Monographs on the Evaluation of the Carcinogenic Risk of Chemicals to Humans Polynuclear Aromatic Compounds: Part 1. Chemical, Environmental, and Experimental Data, International Agency for Research on Cancer, Lyon, France, 1983.

[2] A.M. Jeffrey, K.W. Jennette, S.H. Blobstein, I.B. Weinstein, F.A. Beland, R.G. Harvey, H. Kasai, I. Miura, K. Nakanishi, Benzo[*a*]pyrene–nucleic acid derivatives found *in vivo*: structure of a benzo[*a*]pyrene tetrahydrodiol epoxide–guanisine adduct, J. Am. Chem. Soc. 98 (1976) 5714–5715.

[3] K.W. Jennette, A.M. Jeffrey, S.H. Blobstein, F.A. Beland, R.G. Harvey, I.B. Weinstein, Nucleoside adducts from the *in vitro* reaction of benzo [*a*]pyrene-7,8-dihydrodiol-9,10-oxide or benzo[*a*]-4,5-oxide with nucleoic acids, Biochemistry 16 (1977) 932–938.

[4] M.R. Osborne, F.A. Beland, R.G. Harvey, P. Brookes, The reaction of (±)-7β,8α-dihydroxy-9β,10β-epoxy-7,8,9,10-tetrahydrobenzo[*a*]pyrene with DNA, Int. J. Cancer 18 (1976) 362–368.

[5] M. Koreeda, P.D. Moore, P.G. Wisloki, W. Levin, A. Conney, H. Yagi, D.M. Jerrina, Binding of benzo[*a*]pyrene-7,8-dihydrodiol-9,10-epoxides to DNA, RNA and protein of mouse skin occurs with high stereoselectivity, Science 199 (1978) 778–781.

[6] P.D. Devanesan, N.V.S. RamaKrishna, R. Todorovic, E.G. Rogan, E.L. Cavalieri, H. Jeong, R. Jankpwiak, G.J. Small, Identification and quantitation of benzo[*a*]pyrene–DNA adducts formed by rat liver microsomes *in vitro*, Chem. Res. Toxicol. 5 (1992) 302–309.

[7] E.L. Cavalieri, E.G. Rogan, Central role of radical cations in metabolic activation of polycyclic aromatic hydrocarbons, Xenobiotica 25 (1995) 677–688.

[8] L. Chen, P.D. Devanesan, S. Higginbotham, F. Ariese, R. Jankowiak, G.J. Small, E.G. Rogan, E.L. Cavalieri, Expanded analysis of benzo[*a*]pyrene–DNA adducts formed *in vitro* and in mouse skin: their significance in tumor initiation, Chem. Res. Toxicol. 9 (1996) 897–903.

[9] T.E. Smithgall, R.G. Harvey, T.M. Penning, Spectroscopic identification of *ortho*-quinones as the products of polycyclic aromatic *trans*-dihydrodiol oxidation catalyzed by dihydrodiol dehydrogenase. A potential route of proximate carcinogen metabolism, J. Biol. Chem. 263 (1988) 1814–1820.

[10] L. Floewrs-Geary, W. Bleczinski, R.G. Harvey, T.M. Penning, Cytotoxicity and mutagenicity of polycyclic aromatic hydrocarbon *o*-quinones produced by dihydrodiol dehydrogenase, Chem. Biol. Interact 99 (1996) 55–72.

[11] T.M. Penning, M.E. Burczynski, C.-F. Hung, K.D. McCoull, N.T. Palackal, L.S. Tsuruda, Dihydrodiol dehydrogenases and polycyclic aromatic hydrocarbon activation: generation of reactive and redox active *o*-quinones, Chem. Res. Toxicol. 12 (1999) 1–18.

[12] T.M. Penning, S.T. Ohnishi, T. Ohnishi, R.G. Harvey, Generation of reactive oxygen species during the enzymatic oxidation of polycyclic aromatic hydrocarbon *trans*-dihydrodiols catalyzed by dihydrodiol dehydrogenase, Chem. Res. Toxicol. 9 (1996) 84–92.

[13] M. Shou, R.G. Harvey, T.M. Penning, Reactivity of benzo[*a*]pyrene-7,8-dione with DNA. Evidence for the formation of deoxyguanosine adducts, Carcinogenesis 14 (1993) 475–482.

[14] N. Balu, W.T. Padgett, G.P. Lambert, A.E. Swank, A.M. Richard, S. Nesnow, Identification and characterization of novel stable deoxyguanosine and deoxyadenosine adducts of benzo[*a*]pyrene-7,8-quinone from reactions at physiological pH, Chem. Res. Toxicol. 17 (2004) 827–835.

[15] S. Ding, R. Shapiro, N.E. Geacintov, S. Broyde, Conformations of stereoisomeric base adducts to 4-hydroxyequilenin, Chem. Res. Toxicol. 16 (2003) 695–707.

[16] M.J. Frich, G.W. Trucks, H.B. Schlegel, G.E. Scuseria, M.A. Robb, J.R. Cheeseman, V.G. Zakzewski Jr., J.A. Montgomery, R.E. Stratman, J.C. Burant, S. Dapprich, J.M. Millam, A.D. Daniels, K.N. Kudin, M.C. Strain, O. Farkas, J. Tomasi, V. Barone, M. Cossi, R. Cammi, B. Mennucci, C. Pomelli, C. Adamo, S. Clifford, J. Ochterski, G.A. Petersson, P.Y. Ayala, Q. Morokuma, K. Cui, D.K. Malick, A.D. Rabuck, K. Raghavachari, J.B. Foresman, J. Cioslowski, J.V. Stefanov, B.B. Ortiz, G. Liashenko, A. Liu, P. Piskorz, I. Komaromi, R. Gomperts, R.L. Martin, D.J. Fox, T. Keith, M.A. Al-Laham, C.Y. Peng, A. Nanayakkara, C. Gonzalez, M. Challacombe, P.M.W. Gill, B.G. Johnson, W. Chen, M.W. Wong, J.L. Andres, M. Head-Gordon, E.S. Replogle, J.A. Pople, Gaussian 98. Revision A. 3, Gaussian, Inc., Pittsburgh, PA, 1998.

[17] S.H. Vosko, L. Wilk, M. Nusair, Accurate spin dependent electron liquid correlation energies for local spin density calculations: a critical analysis, Can. J. Phys. 58 (1980) 1200–1211.

[18] C. Lee, W. Yang, R.G. Parr, Development of the Colle–Salvetti correlation-energy formula into a functional of the electron density, Phys. Rev., B 37 (1988) 785–789.

[19] A.D. Becke, Density functional exchange-energy approximation with correct asymptotic behavior, Phys. Rev., A 38 (1988) 3098–3100.

[20] A.D. Becke, Density functional thermochemistry: III. The role of exact exchange, J. Chem. Phys. 98 (1993) 5648–5652.

[21] J. Tan, N.E. Geacintov, S. Broyde, Principles governing conformations in stereoisomeric adducts of bay region benzo[*a*]pyrene diol epoxides to adenine in DNA: steric and hydrophobic effects are dominant, J. Am. Chem. Soc. 122 (2000) 3021–3032.

[22] J. Tan, N.E. Geacintov, S. Broyde, Conformational determinants of structures in stereoisomeric *cis*-opened anti-benzo[*a*]pyrene diol epoxide adducts to adenine in DNA, Chem. Res. Toxicol. 13 (2000) 811–822.

[23] X.-M. Xie, N.E. Geacintov, S. Broyde, Stereochemical origin of opposite orientations in DNA adducts derived from enantiomeric anti-benzo[*a*] pyrene diol epoxides with different tumorigenic potentials, Biochemistry 38 (1999) 2956–2968.

[24] X.-M. Xie, N.E. Geacintov, S. Broyde, Origins of conformational differences between *cis* and *trans* DNA adducts derived from enantiomeric *anti*-benzo[*a*]pyrene diol epoxides, Chem. Res. Toxicol. 12 (1999) 597–609.